THIRTEENTH EUROPEAN ROTORCRAFT FORUM

1.2

Paper No. 71

MEASURED AND PREDICTED IMPULSIVE NOISE DIRECTIVITY CHARACTERISTICS

K.J. Schultz and W.R. Splettstoesser

D F V L R
Institute for Design Aerodynamics
3300 Braunschweig, Germany

September 8-11, 1987

ARLES, FRANCE

ASSOCIATION AERONAUTIQUE ET ASTRONAUTIQUE DE FRANCE

MEASURED AND PREDICTED IMPULSIVE NOISE DIRECTIVITY CHARACTERISTICS

K.J. Schultz and W.R. Splettstoesser

DFVLR, Institute for Design Aerodynamics
3300 Braunschweig ,FRG

Abstract

The prediction of radiated high-speed and blade/vortex-interaction impulsive noise from a helicopter rotor in forward flight condition requires a detailed knowledge of the aerodynamic sources, characterized by highly unsteady transonic flow fields and blade surface pressures, respectively. Since such information is not available from exclusively theoretical approaches, measured model-rotor blade pressure data - together with a semi-empirical relation combining the blade surface pressures with a "momentum-thickness"- are used as source input data for a non-compact prediction code, including all of the three source terms of the"Ffowcs-Williams/Hawkings-equation". The measured blade pressure data serve as direct input for the loading term and is further used in a more indirect manner to calculate an approximated quadrupole term by means of the "momentum thickness" which is considered as an essential quadrupole parameter. The predicted impulsive noise characteristics(wave forms) are compared with acoustic data, that had been measured simultaneously with the blade pressure data. Good agreement in amplitude , wave form and directivity is demonstrated for two forward-flight high-speed conditions and for a typical BVI- condition.In addition the complete directivity pattern was numerically calculated for (a) the vertical plane through the rotor axis for both HS- and BVI- flight conditions, (b) for the rotorplane for a HS-case and (c) for a horizontal plane underneath the rotorplane for a typical BVI-case. Thus, the strong inplane-upstream directivity for the HS-test condition as well as the dynamic development of advancing side and retreating side BVI for the BVI-condition is demonstrated.

1. Introduction

Rotor impulsive noise, the most annoying and also highly detectable contributer to helicopter noise radiation has recently become subject of intensive experimental and theoretical research. Meanwhile it is wellknown that impulsive noise, also called "blade slap",is caused by two different phenomena. One of them, termed "blade/vortex-interaction " (BVI) impulsive noise, is characterized by the acoustic radiation from highly unsteady blade surface pressure fields, occuring when the blade interacts with previously shed and rolled-up tip vortices. Each encounter on the advancing side causes a positive pressure peak, when measured in an upstream/downward observer position. The second phenomenon,termed high speed (HS) impulsive noise(sometimes also referred to as "compressibility/thickness noise"),is characterized by acoustic radiation from unsteady transonic flow fields in the advancing rotor blade's tip region at high tip Mach-numbers, resulting in pronounced negative pressure peaks, that are "beamed" in an upstream-inplane direction.

The theoretical basis for rotor noise prediction is the wellknown general integral equation governing the noise radiation from moving surfaces,usually referred to as "Ffowcs Williams/Hawkings(FWH) -equation",which is a special

application and extension of Lighthills acoustic analogy (Ref.1) and is provided for numerical calculation of rotor noise by Farassat(Ref.2). It comprises three source terms (1) thickness(monopole) term, (2) loading (dipole) term and (3) quadrupole term and requires detailed knowledge of the very complex rotor blade aerodynamics as source input.

For BVI impulsive noise the loading term is most important, while the HS-impulsive noise depends mainly on the thickness term and at high tip Mach-numbers on the quadrupole term. Therefore previous theoretical investigations were concentrated either on BVI- or on HS-impulsive noise. Initial approaches by Boxwell,Yu and Schmitz(Ref.3) and also Farassat,Nystrom and Morris(Ref.4) were focussed on the inplane highspeed impulsive noise at hover. But because of neglecting the quadrupole term at high tip Mach-numbers these first approaches have failed to accurately predict amplitude and wave form of very carefully measured HS-impulsive noise data(Ref.3). Just recently Brentner(Ref.5) has used a new computer code (WOPWOP) to predict cases of helicopter rotor noise, including a moderate speed forward flight case, but also neglecting the quadrupole term. The required blade pressures were obtained theoreticaly by the C81- computer code.Again the comparison with experimental data has shown not quite satisfactory agreement. Yu,Caradonna and Schmitz(Ref.6) have improved the prediction accuracy by incorporating the nonlinear quadrupole term and achieved better results up to tip Mach-numbers of about 0.9 for the inplane hovering impulsive noise(Ref.7), however with a considerable overprediction at higher Mach-numbers. Using a frequency domain method to predict transonic quadrupole rotor noise in hover was presented by Prieur(Ref.8), with good results. In both cases the source aerodynamic characteristics were obtained numerically by transonic small disturbance potential codes(Ref.9 and 10).

However, a complete numerical simulation of the highly unsteady three-dimensional transonic flow field of a rotor in forward flight is not available, especially with a realistic simulation of BVI.Therefore until now the rotor noise prediction is depending on experimental rotor blade aerodynamic data as source input.

A first attempt to predict BVI-signatures of a rotor in descending flight was made by Nakamura (Ref.11) using measured blade pressure data from a joint U.S. Army/Bell Helicopter Textron flight test program. He only considered the linear loading term of the FWH-equation . Because of an obviously unsufficient interpolation scheme for modeling the limited number of measured blade pressure data for the numerical calculation the agreement of the BVI wave forms with simultaneously measured noise data was rather poor. Similar blade vortex interaction noise predictions using measured blade pressures and only linear source terms were recently published by Ziegenbein and Oh(Ref.12) and also Joshi,Liu and Boxwell(Ref.13), again with limited agreement of prediction and measurement.

However,in general,the idea of using experimental rotor blade aerodynamic data for impulsive noise prediction is worthwhile to be pursued, as has been shown by the authors in Ref.14. Here a new attempt was presented to use measured blade pressures as source input for a prediction method, which includes all of the three source terms of the FWH-equation. Whilst the calculation of the thickness term can be performed as developed in Ref.2 and 15, for the calculation of the loading term and the quadrupole term some further considerations were necessary. Because the number of measuring points will always be less than necessary, a special interpolation scheme was developed to obtain a sufficient blade pressure information for all blade panels. The

blade pressure distribution was used not only for the loading term, but also in a more indirect manner to calculate an approximated quadrupole term.

The prediction method was successfully tested using well-documented hovering impulsive noise data and then applied to one descending flight condition with strong BVI-activity and for two forward flight high- speed conditions. Encouraged by the good agreement of predicted and measured acoustic wave-forms, documented in Ref.14, in the present paper for the same test cases the complete directivity pattern is being calculated and presented. The waveforms also shown for directions where no measured data are available, allow the tracing of the development and disappearence of advancing and retreating side BVI. To begin with, the most important features of the prediction method are described and some comparisons of predicted and measured wave-forms are shown.

2. Basic theory and prediction scheme

The subject problem is mathemathically described by the following integral equation governing the noise radiation from moving sources:

$$4\pi p'(\vec{x},t) = \frac{\partial}{\partial t}\int_S \left|\frac{\rho_o v_n}{r|1-M_r|}\right|_{ret.} dS(\vec{y}) - \frac{\partial}{\partial x_i}\int_S \left|\frac{P_{ij}n_j}{r|1-M_r|}\right|_{ret.} dS(\vec{y}) + \frac{\partial^2}{\partial x_i \partial x_j}\int_V \left|\frac{T_{ij}}{r|1-M_r|}\right|_{ret.} dV(\vec{y}). \quad (1)$$

The sound pressure p' at time t on an observer position $\vec{x}$ depends on three source integral terms, radiating from the source location $\vec{y}$ at the retarded time τ. M_r is the source Mach-number component in observer direction, r is the observer-source distance, vn is the velocity disturbance normal to the blade surface, p_{ij} is the stress-tensor and T_{ij} is the "Lighthill-tensor". The effect of moving sources is accounted for by the Doppler-amplification factor $1/(1-M_r)$.

This equation was originally derived by Ffowcs-Williams and Hawking(s.Ref.1, therefore often called FWH-equation) and modified be several researchers,especially by Farassat(Ref.2). The three source integrals are acoustically classified after Lighthills analogy as monopole, dipole and quadrupole. With regard to its physical meaning the monopole is called the "thickness term", and the dipole is called "loading term". The quadrupole term is much more complex,since this volume integral includes the complete perturbated flow field, expressed by the Lighthill-tensor T_{ij} :

$$T_{ij} = \rho u_i u_j + P_{ij} - a_o^2 \rho \delta_{ij} \quad (2)$$

The present prediction code uses the following formulation, which includes the so-called loading near-field term(Ref.2):

$$4\pi p'(\vec{x},t) = \frac{\partial}{\partial t}\int_S \left|\frac{\rho_o v_n}{r|1-M_r|}\right|_{ret.} dS(\vec{y}) + \frac{1}{a_o}\frac{\partial}{\partial t}\int_S \left|\frac{P_r}{r|1-M_r|}\right|_{ret.} dS(\vec{y})$$

$$+ \int_S \left|\frac{P_r}{r^2|1-M_r|}\right|_{ret.} dS(\vec{y}) + \frac{1}{a_o^2}\frac{\partial^2}{\partial t^2}\int_V \left|\frac{T_{rr}}{r|1-M_r|}\right|_{ret.} dV(\vec{y}). \qquad (3)$$

Very recently Farassat and Brentner(Ref.16) have completed the formulation with additional quadrupole terms,but too late to be considered in this state. The spatial differentiation is converted into a time differentiation. The subscript r means source-observer direction. Thus the source input P_r corresponds directly to the blade surface pressure or equivalent to the loading vector contribution in the source-observer direction and measured blade pressures can be used directly. The quadrupole source input T_{rr} will be considered in detail later on.

In the numerical approach the noise received at an observer position and at observer time(or during some time period) can be interpreted as a superposition of many individual noise contributers, each radiating at their individual retardet times from their individual positions. Thus the blade surface (or the surrounding volume) can be divided into a suitable number of source panels, i.e. small" compact sources" with their respective source characteristics at the retardet time. In the subject case the considered time period is one rotor revolution. It was found that an appropriate time increment for impulsive noise prediction is 1/512(better 1/1024) of a revolution. The chord is divided into 21 and the span into 18 segments in the 50% to 100 % region. The discretization on the leading edge and at the blade tip is the finest, of cource. In addition for the quadrupole term about 10 out- of-tip spanwise locations were used. The noise radiation from the upper and lower side is calculated separately. Usual calculations with a differential loading input normal to the blade chord neglect the influence of the real blade surface normal direction, especially near the leading edge. This may contribute to an unsatisfactory result.

3. Blade pressure interpolation scheme

The experimental data used as source input for the numerical prediction and the acoustic comparison, resp., originate from the joint US-Army/DFVLR model rotor test in the German Dutch Windtunnel (DNW) (Ref.17,18and19),where a 1/7 scale AH-1/OLS model rotor was run in the DNW 6*8m open jet configuration characterized by excellent flow and anechoic proporties, as well as low back-ground noise(Ref.20).

During these tests, an extensive base of experimental data for both high-speed and blade/vortex-interaction impulsive noise radiation was obtained, including simultaneously measured blade pressures.This was possible because one of the rotor blades was instrumented with 32 flush mounted Kulite absolute pressure transducers. Fig. 1 shows the arrangement of the transducer positions in the blade tip region. Unfortunately,not all of the transducer signals have been recorded. Thus, use could be made of one row on the very leading edge(3% chord) in the spanwise direction and of another row at an outer span position (about 97% radius) in chordwise direction, each on the upper and on the lower side.

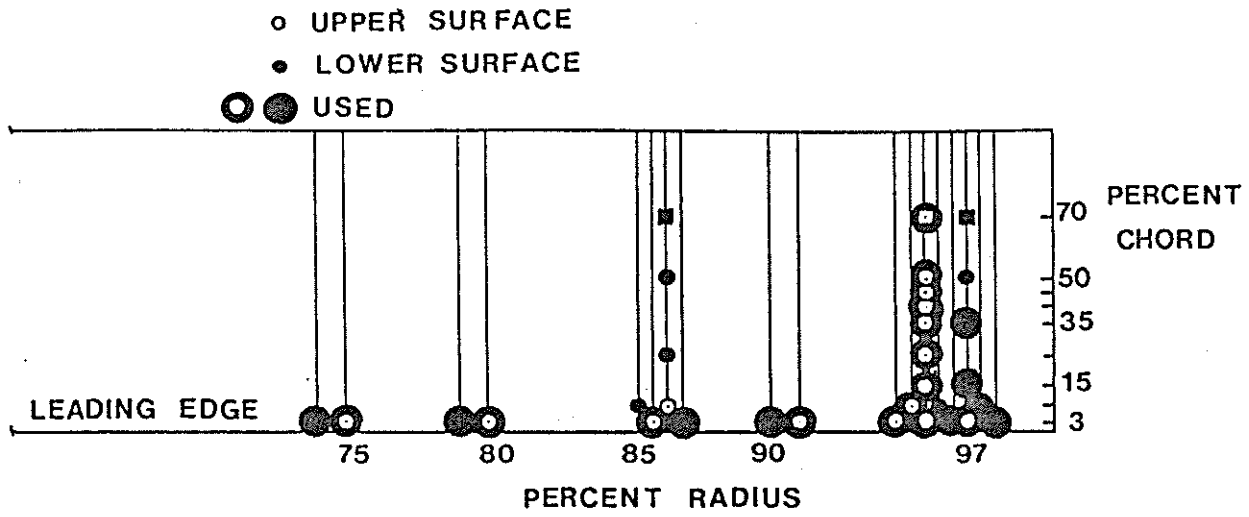

Fig.1: Absolute pressure transducer locations on the AH-1/OLS model rotor blade

Fig. 2a) shows measured spanwise and Fig 2b) chordwise pressure time histories for the investigated BVI-case (descending flight condition) on the upper and on the lower side. Fig. 2b) indicates that BVI induced pressure peaks are only important up to about 15% chord.

Fig. 3 a) and b) present for the same positions the pressure signatures for the investigated moderate HS-case(advancing tip Mach-number of 0.84) ,and Fig 4 a) and b) for the increased HS-case(advancing tip Mach-number of 0.894). Minor BVI signatures are still visible and have to be included in the noise prediction.

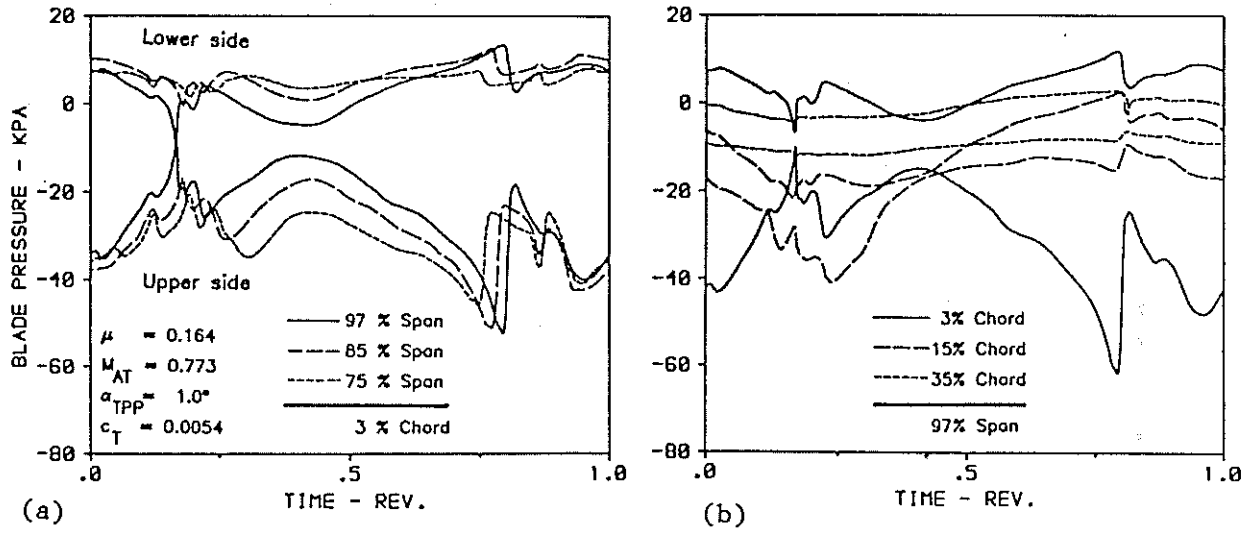

Fig.2: BVI blade surface pressure time histories, a) near the leading edge(3% chord) at different span positions, b) in the outer tip region(97% radius) at different chord locations

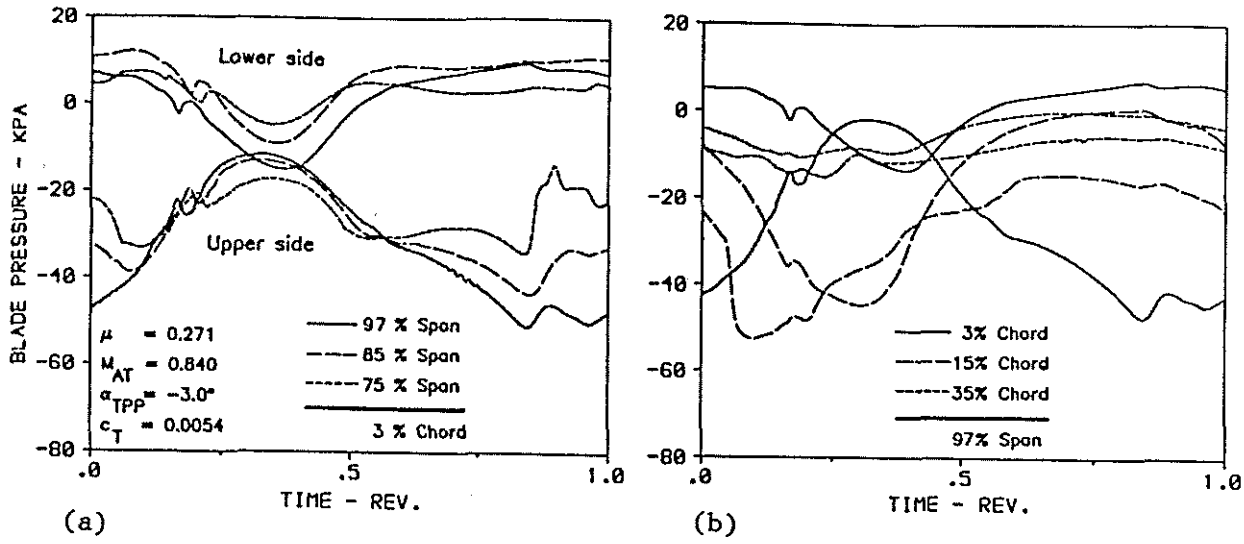

Fig.3: HS blade surface pressure time histories at moderate advancing tip Mach-number, a) near the leading edge(3% chord) at different span positions, b) in the outer tip region(97% radius) at different chord locations

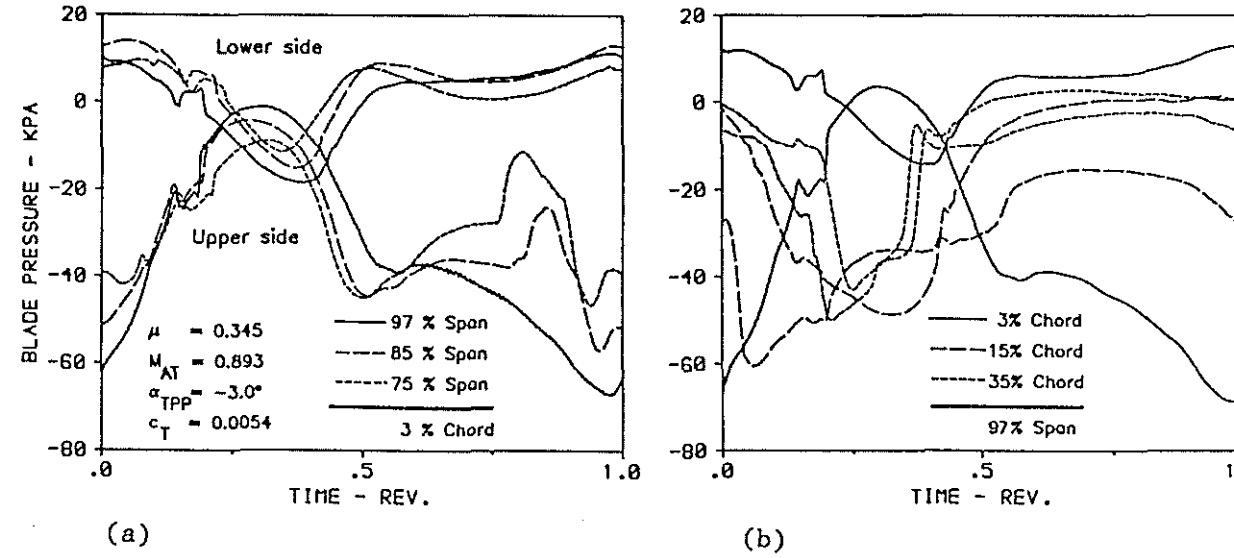

Fig.4: HS blade surface pressure time histories at high advancing tip Mach-number, a) near the leading edge(3% chord) at different span positions, b) in the outer tip region(97% radius) at different chord locations

It is obvious that only for a limited number of panels the measured data can be used directly. For all other panels, the measured blade pressures in the vicinity must be interpolated or extrapolated in a suitable way, without loosing the BVI phase information. Fig. 5a) shows a typical BVI blade pressure time history, subdivided into several segments, which are separated by the BVI-peaks. Because the peaks, indicating interactions,have a certain time delay (phase shift) between different locations on the blade surface, each segment has to be interpolated separately, that means, the interpolation has to be carried out not only for the amplitudes, but also for the time coordinate, which corresponds to the azimuth angle. If an interpolation between the time histories of two measuring points is required to determine the time

history of an intermediate panel the new interaction (peak) points and thus the new segment length were determined first. The segments of the two adjoining time histories were then stretched or compressed into the new segment length before interpolating the amplitudes. Thus the phase information was preserved and the important BVI-peaks were not smoothed out.

In Fig 5b) all of the measured spanwise peak locations were plotted in the rotor plane, forming BVI trajectories. The lines were obtained from approximated (epicycloide) BVI trajectory calculations and used for extrapolation purposes. To complete the spanwise pressure input up to 100% span and down to 50% span, the measured blade pressures were extrapolated making use of theoretical considerations and experimental experience. In a similar way, the pressure profiles in chord direction were inter- and extrapolated using the dynamic pressure on the leading edge as additional information.

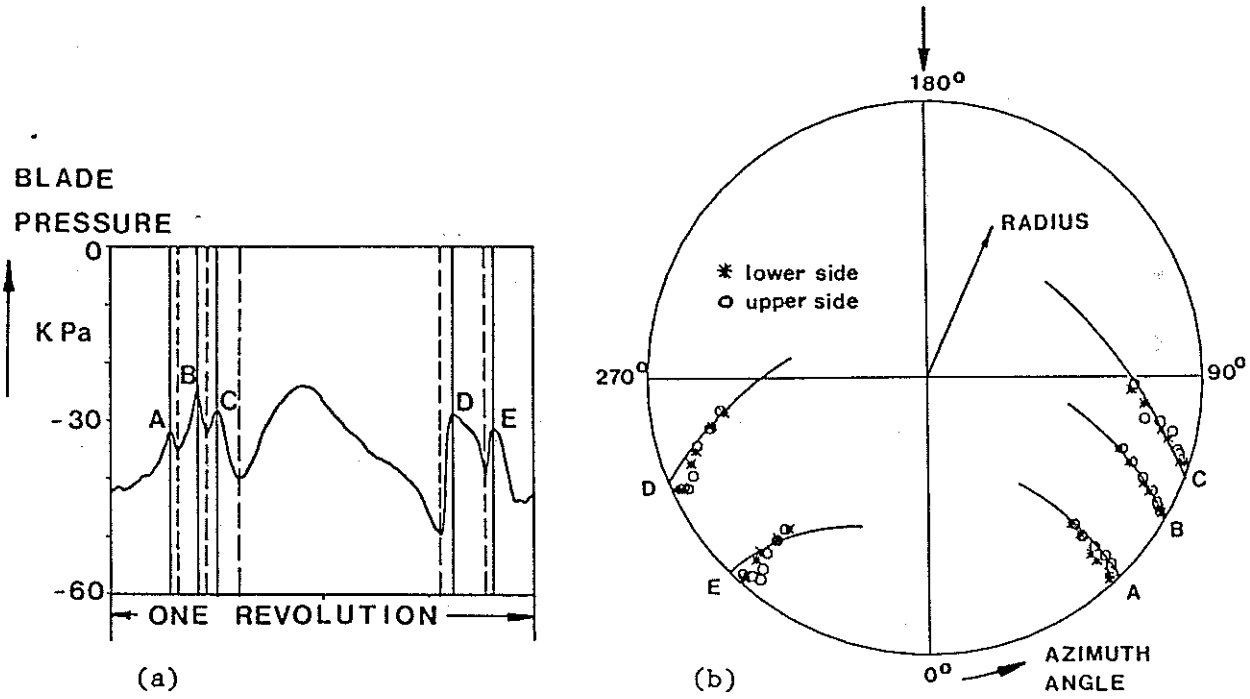

Fig.5: Blade pressure interpolation, a) Example for BVI peaks in the time history as per subdivision markings, b) measured spanwise peak locations and approximated BVI encounter trajectories in the rotor plane

In the preceeding step a complete spanwise (at 3% chord) and a complete chordwise (at about 97% span) pressure time history characteristic was obtained. The next step now is to superimpose the spanwise characteristic on the chordwise characteristic for each panel. This concerns mainly the blade vortex interaction azimuth angles. With regard to the amplitudes up to 3% chord the spanwise characteristics were taken ,above 3% chord it was assumed that the chordwise pressure profile measured at the 97% span location is sufficiently similar on the entire outer span regime of interest. The degree of accuracy decreases towards the inner span/trailing edge direction. Fortunately the contribution to the total noise radiation decreases in the same way. At the most contributing regimes the pressure input is considered to be quite accurate.

To exclude the random part in the blade pressure time histories (and in so far removing the broad band noise part, which is not subject of the present investigation), averaged pressure time histories were used to yield numerical results, which were then compared with averaged measured sound pressure time histories.

4. Quadrupole approximation

The idea of quadrupole approximation , originally introduced by Yu,Caradonna and Schmitz(Ref.6) is to reduce the Lighthill-tensor volume integral into an easier to handle surface integral. The main part of the Lighthill-tensor T_{ij} is the momentum flux tensor u_{ij} . With the usual aerodynamic slender body approximation (small disturbances) it can be written as

$$\rho u_i u_j \approx \rho u_s^2 \tag{4}$$

whereby u is the streamwise perturbation velocity. If isentropic flow is assumed the Lighthill-tensor T_{ij} can be approximated by

$$T_{ij} \approx \rho_o u^2 \left(1 + \frac{\varkappa - 1}{2} M_o^2\right) \tag{5}$$

which is proportional to the square of the streamwise perturbation velocity. M_o is the free stream Mach-number and κ is the specific heat ratio(1.4 for air).

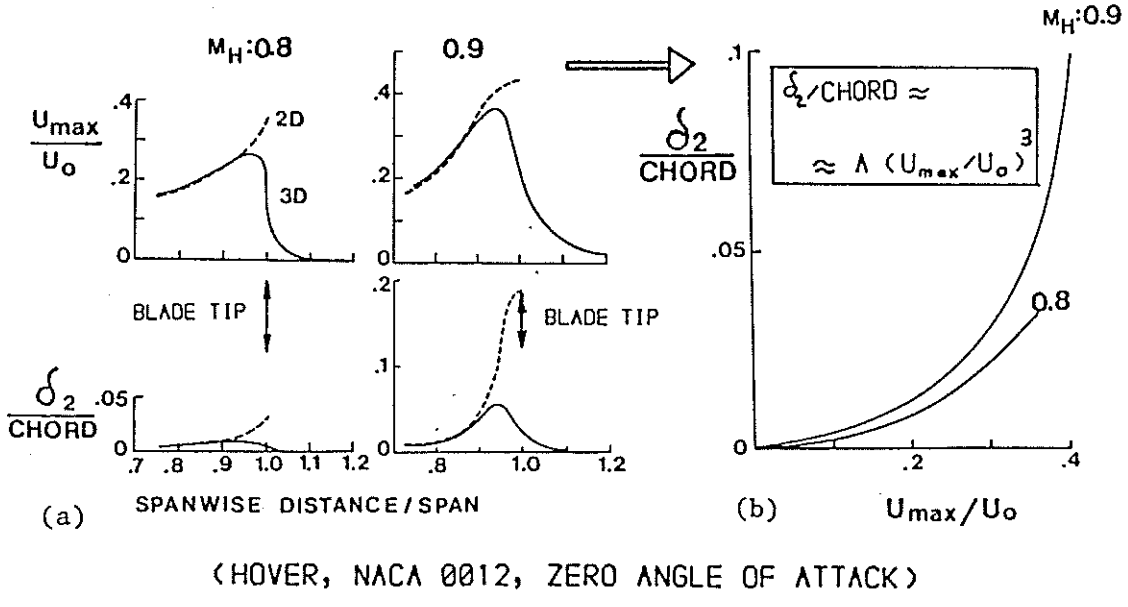

Fig.6: Quadrupole approximation, a) maximum perturbation velocity and momentum thickness vs. span distance(from Ref.6), b)semi-empirical relation for the momentum thickness

Assuming the volume of effective perturbation velocity to be limited to a region near the surface, the volume integral can be splitted into an integral in the direction normal to the surface and into a surface integral. Caradonna et al (Ref.6) have introduced a so-called "momentum thickness"

$$\delta_2 = \int_n \left(\frac{u}{u_o}\right)^2 dn \qquad (6)$$

The quadrupole volume integral, considered for farfield radiation in the observer direction may then be approximated by the following surface integral:

$$\frac{1}{a_o^2}\,\frac{\partial}{\partial t^2}\int_V \left|\frac{T_{rr}}{r|1-M_r|}\right|_{ret.} dV = \frac{\partial}{\partial t^2}\int_S \left|\frac{\delta_{2r}}{r|1-M_r|}\,\rho_o M_o^2\,(1+\frac{\kappa-1}{2})\right|_{ret.} dS. \qquad (7)$$

Caradonna et al have calculated the unknown momentum thickness distribution with their transonic small disturbance potential equation computer code(Ref.9). Fig.6a shows the results for the maximum perturbation velocity on the surface and the momentum thickness along the blade span for tip Mach-numbers of 0.8 and 0.9. The idea of the present approach is to use the measured blade pressure data also for the quadrupole approximation, considering (1) the maximum streamwise perturbation velocity at the surface to be coupled by the Bernoulli equation with the blade surface pressure, and (2) the relationship between the surface perturbation velocity and the momentum thickness is known. The latter may be a complex function depending on Mach-number, angle of attack and blade geometry, but the idea was, that a more generally valid relation may be found from the rotor flow field prediction, and that the most important information,especially the unsteady characteristics, are included in the measured blade pressures. In a first attempt a relation was used, which was obtained from the results of Caradonna et al(Ref.6) In Fig. 6b the $\delta 2$ -values for the tip Mach-numbers 0.8 and 0.9 are plotted versus the surface perturbation velocities, as obtained from Fig. 6a . It appears , that a general relation exists for this particular blade (NACA 0012) which can be expressed by

$$\delta_2/\text{CHORD} \approx A\,(u_{max}/u_o)^3 \qquad (8)$$

with A=1.4 for the tip Mach-number 0.9. It is assumed that this approximation is also valid for the considered AH-1/OLS-model blade airfoil, which is not very different from the NACA 0012 airfoil. Also the blade tip is rectangular in both cases and the aspect ratio is similar.It is further assumed,that the relation ,obtained for a hover case is similar in the forward flight case with similar tip Mach-number at the considered source position. The applied procedure is a first order approximation at this state, but might be improved or better still replaced by exactly calculated aerodynamic results, if available at a later date.

A further relation, concerning the decrease of the momentum thickness from its maximum at about 95% span, where the chordwise measurements were taken, to the outer-span and out-of-tip region,was directly obtained from Fig. 5a). This strongly Mach-number dependent relation considers the three- dimensional effect on the said momentum thickness in the near-tip and out-of-tip region.

Allthough this crude approximation of the quadrupole term is not an optimum - in comparison to the earlier predictions (only including thickness and loading term) the improvement is considerable, especially for the high speed

case, but also for out-of-rotor-plane locations which were not considered in the work of Caradonna et al.

5. High speed impulsive noise results

At first the prediction scheme was applied to the relatively uncomplicated case of impulsive noise at hover - uncomplicated in so far as no unsteadiness is involved. The blade pressures are not a function of the rotor azimuth angle. The blade pressure profiles for the hover condition were quite repeatably measured and also calculated. The known steady chordwise blade pressure distribution for a NACA 0012 airfoil at different Mach-numbers and its three-dimensional span dependence was used (taken from Refs.6 and 7) as input for the loading term and also for the momentum-thickness approximation in the way described above. Fig.7 shows the excellent agreement between the predicted and the measured noise radiation, even at a tip Mach-number of 0.9, where a shock is visible in the acoustic pressure time history. The wave-forms as well as the power spectra are almost identical over a wide range of tip Mach-numbers. It is interesting to note that the higher harmonic content dramatically increases at higher Mach-numbers about 0.9, an explanation of the severe (subjective) annoyance of highly impulsive noise.

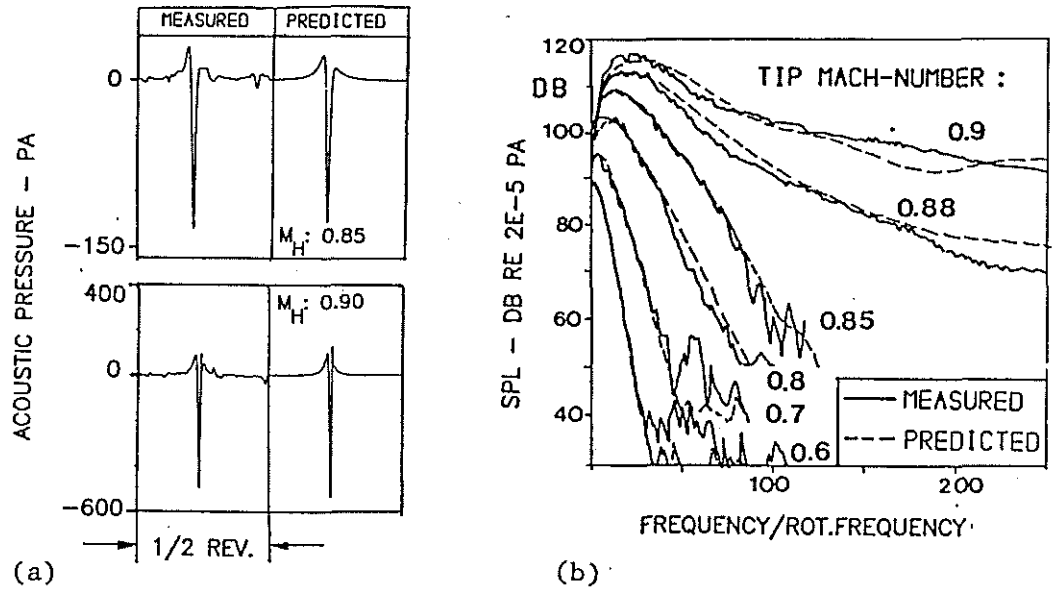

Fig.7: Comparison of experimental and predicted wave forms (a) and power spectra envelopes (b) for different tip Mach-numbers at hover condition

Encouraged by the excellent agreement between measured and predicted results in the hover case an attempt was made to apply the prediction method also to the forward flight case. In Fig.8 the measured and predicted signatures for 6 in-flow microphone locations at a moderate high speed condition for an advance ratio of 0.27 (advancing tip Mach-number of 0.84) are compared. In each case only one event is shown occuring within the time frame of 1/2 rotor revolution. It is obvious that also in forward flight a BVI-contribution is present in every time history. Taking the measured unsteady blade pressure distribution for a full rotor revolution into account, the characteristic

unsteady BVI-contribution is also included in the noise prediction, and the comparison of prediction and experiment is very good in amplitude, wave-form shapes, and even pulse widths. Slight differences at some locations may be explained by slight inaccuracies of the extrapolated blade pressure input and/or by an influence of the rotor downwash, not considered in the noise propagation calculation of the prediction scheme. The in-plane radiation is dominated by the thickness and momentum-thickness terms, while for the out-of-plane radiation the unsteady loading term becomes equally important. This was more clearly demonstrated in Ref.14, where the individual contributions of the three source terms were singled out.

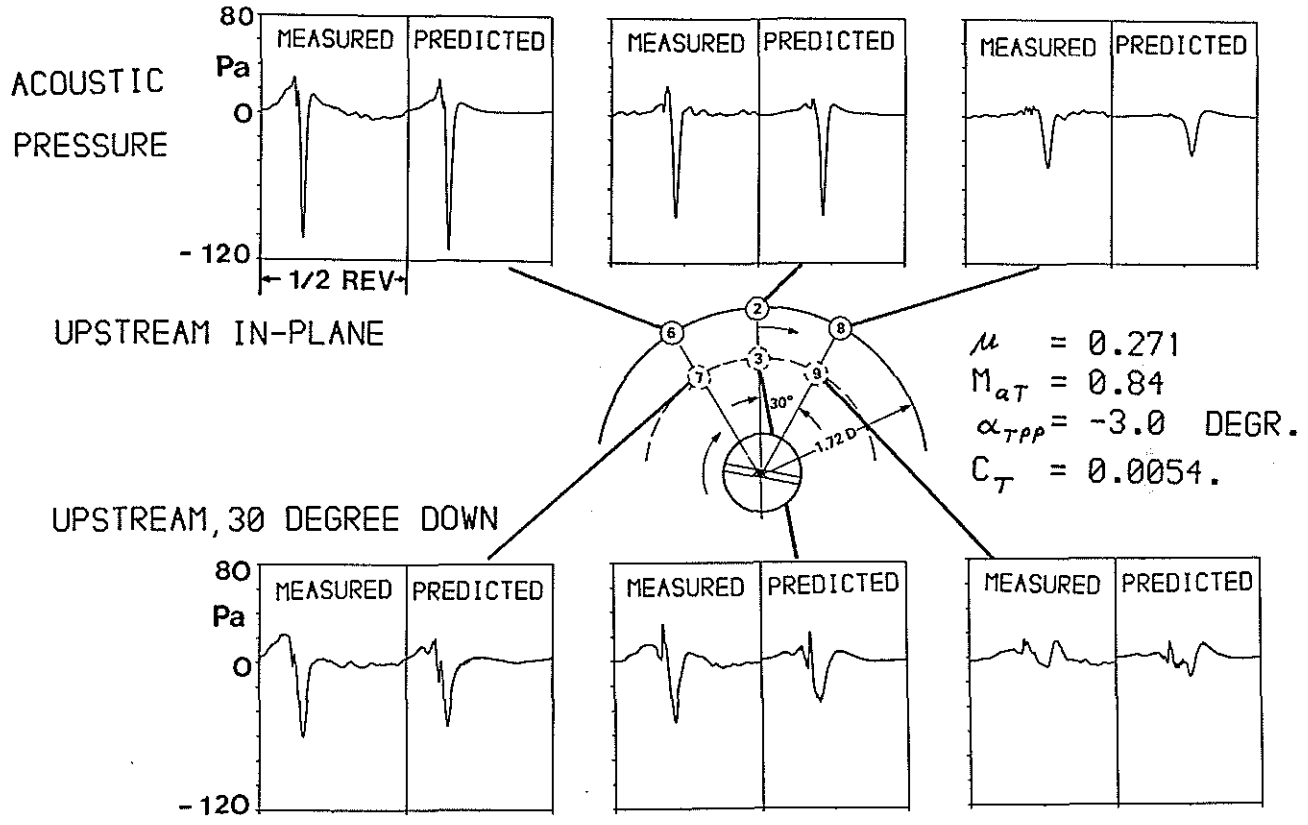

Fig.8: Comparison of experimental and predicted impulsive noise wave forms (moderate high speed condition)

The comparison of measured and predicted acoustic pressure signatures for the high advance ratio of 0.34 (advancing tip Mach-number of 0.89) is shown in Fig.9. Again very good agreement of prediction and measurement is obtained. The in-plane high-speed noise peak pressures have increased considerably and at the in-plane microphones on the advancing side the shock-like pressure rise is well predicted. But Fig.9 also shows that an additional effect must take place,not included in the present prediction, because the negative peak pressure is overpredicted at the advancing side and underpredicted at the retreating side.

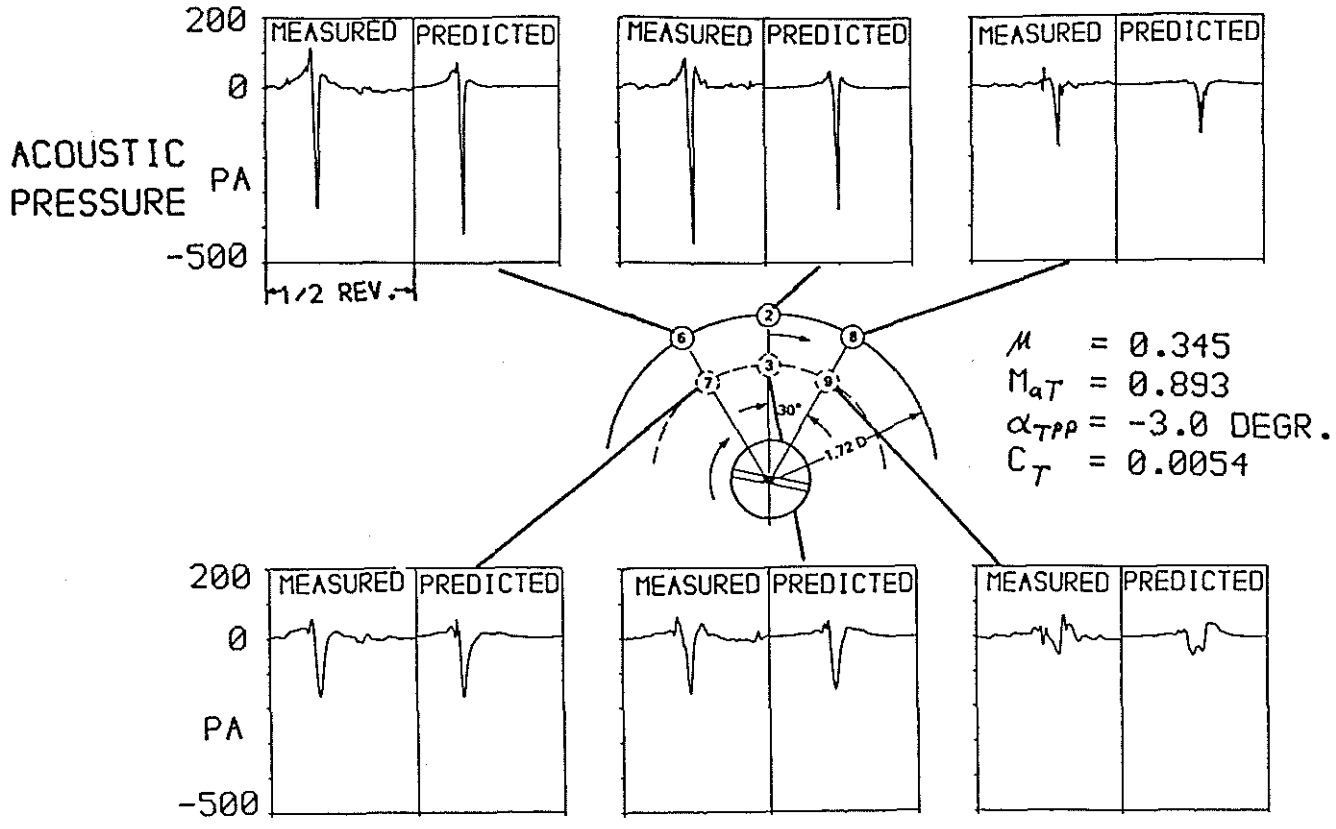

Fig.9: Comparison of experimental and predicted impulsive noise wave forms (high speed condition)

The difference in the measured and predicted directivity is more clearly shown in Fig.10, where in steps of 15 degrees for the entire rotor plane the time histories for 1/2 rotor revolution are shown. In the center the negative peak pressure amplitudes are drawn in form of a polar diagram, enhancing the directivity pattern. The time histories shown are taken from a HS-case with a high advancing tip Mach-number of 0.894, to show the waveform dependence versus the in-plane azimuth angle.

The comparison of the predicted and measured directivity lobes shows a certain difference in the azimuth angle for the maximum amplitude at higher advancing tip Mach-numbers.The measured maximum peak pressure is found more towards the central upstream direction. This may be explained by the neglecting of the real near-field aerodynamics(downwash) and by blade dynamic effects, as for example the unsteady lead lag motion, not included in the prediction. Another possible explanation may be obtained following the statment of Prieur (Ref.8), that the radial velocity disturbance in the quadrupole term (u_r u_s and u_r u_r, not considered in the present prediction), might contribute up to about 15%. This is dependent on the azimuth angle and may affect the directivity. Also the additional quadrupole terms, given by Farassat and Brentner(Ref.16) might have an effect on directivity and amplitude. Therefore further investigations should try to clarify the quadrupole contribution in more detail.

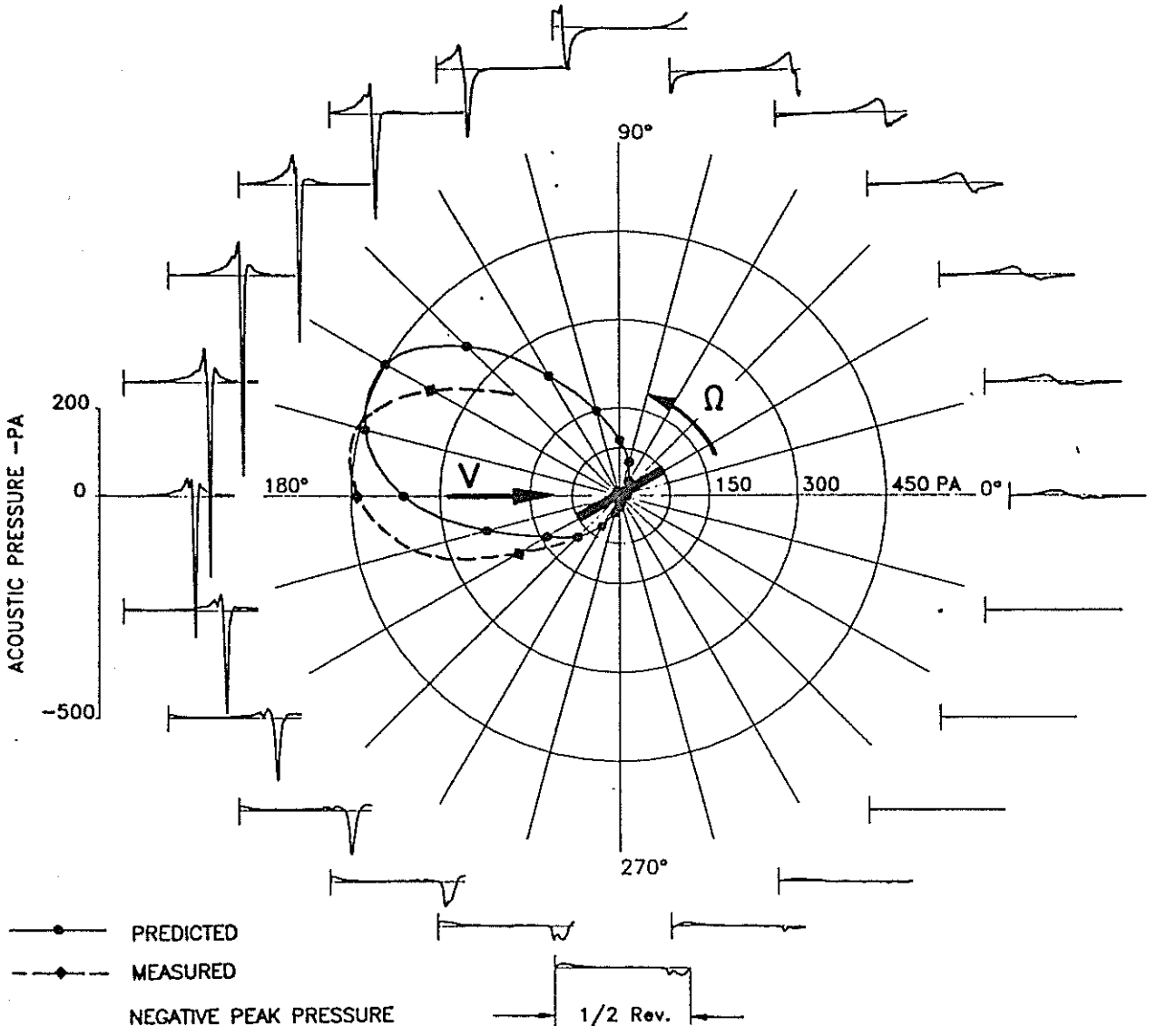

Fig.10: Predicted in-plane directivity characteristics at high speed condition (as in Fig.9)

Fig. 11 shows the longitudinal directivity characteristics in the central vertical plane through the rotor axis. The strong in-plane radiation of HS noise is nicely demonstrated.In out-of-plane directions also the loading term contributes considerably to the negative impulse. At angles greater than 30 degrees it is even the only effective term for the out-of-plane radiation.

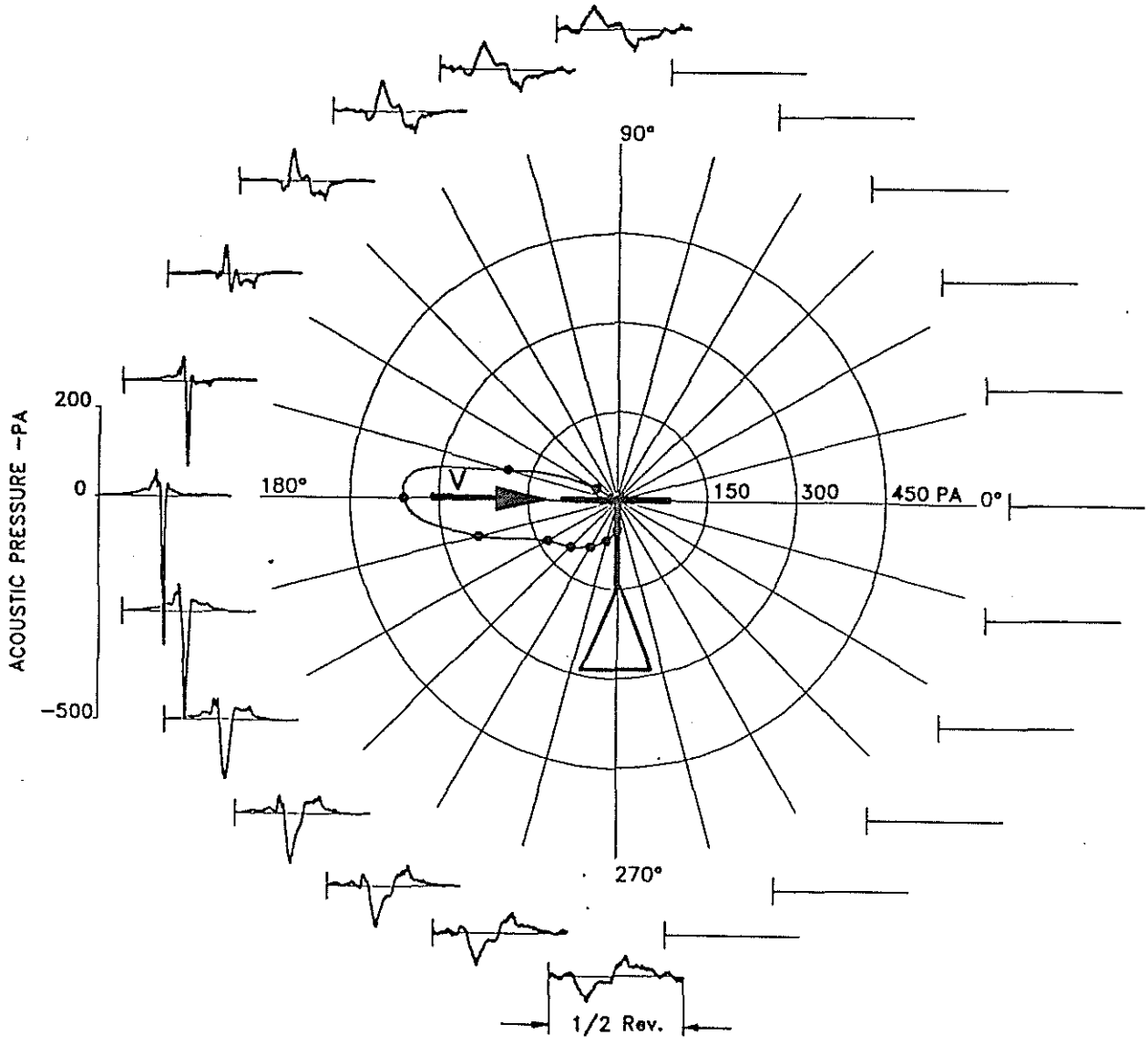

Fig.11: Predicted longitudinal directivity characteristics vertical to the rotor plane at high speed condition (as in Fig.9)

6. BVI impulsive noise results

For the prediction of BVI impulsive noise the unsteady blade pressure distribution as input to the loading term is most important. The blade pressure time histories, used in the present BVI noise prediction (as shown in Fig.3), indicate three BVI peaks on the advancing side and two on the retreating side. The comparison of the predicted and measured noise radiation is shown in Fig.12 for identical observer locations as in the HS-case. The comparison of predicted and measured acoustic wave-forms is very satisfactory and at least as good as the agreement between measured model rotor and full-scale results, published earlier in Ref.17. Also the directivity characteristics of the BVI-impulsive noise are well predicted with only some differences at the in-plane retreating side and on the out-of-plane advancing side.

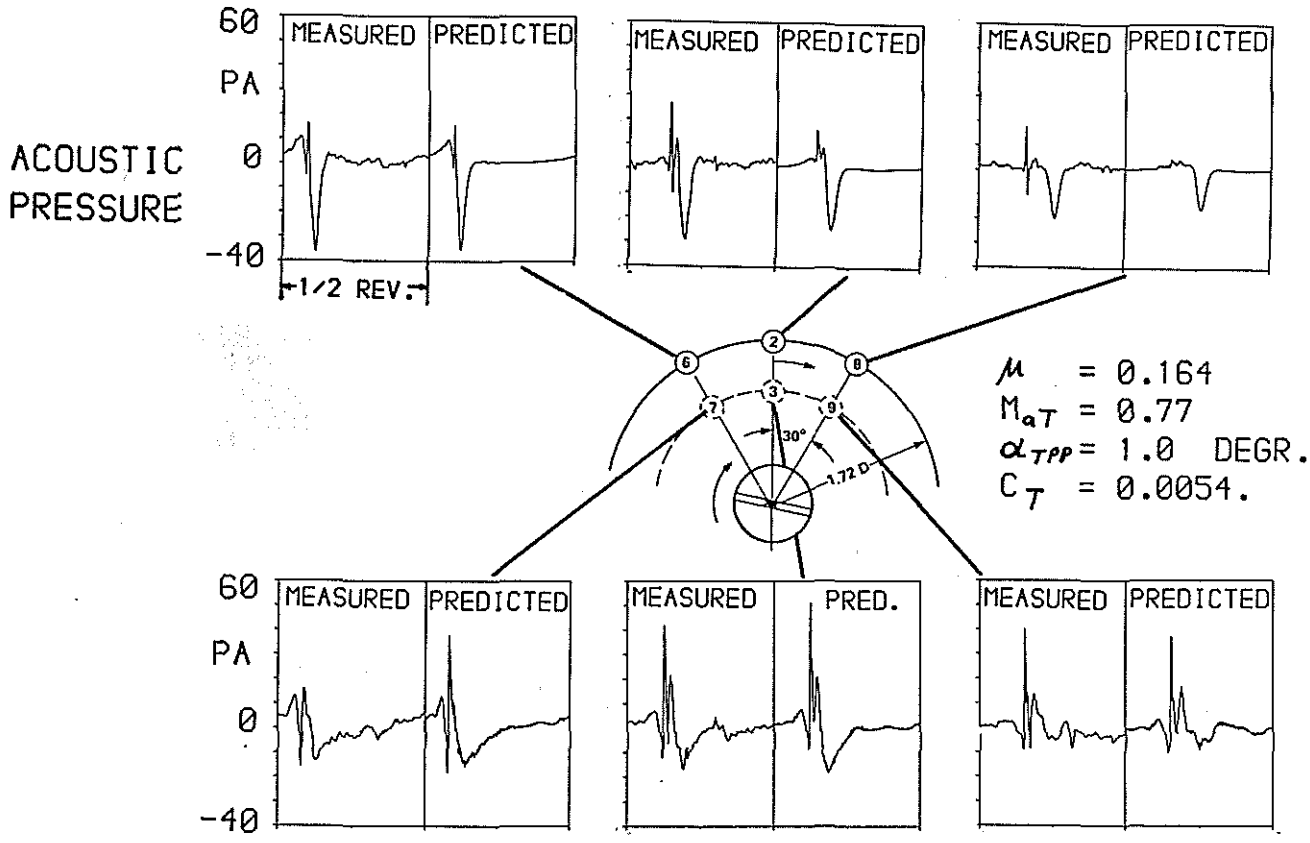

Fig.12: Comparison of experimental and predicted impulsive noise wave forms (Blade vortex interaction condition)

The individual contributions of the three source terms to the total BVI impulsive noise wave-form for in-plane and out-of-plane radiation has been singled out in Ref.14. The out-of-plane radiation (about 20 to 60 degrees) is clearly dominated by the loading term, and for the in-plane radiation the thickness term is most important. The results clearly demonstrates that even at this moderate advancing tip Mach-number the quadrupole term should not be neglected. In the in-plane radiation direction the quadrupole term intensifies not only the negative peak pressure , but also the BVI peaks, because the unsteady blade pressures, used for the quadrupole calculation, lead also to unsteady quadrupole contributions.

Retreating side BVI, recently often discussed, is not visible at the upstream observer positions, where due to the employed microphone arrangement a comparison with measurements is possible. However, the numerical calculation for downstream locations shows very well the development of retreating side BVI. This is demonstrated in Fig.13, where the time histories (waveforms) for 1/2 rotor revolution are plotted for the entire central vertical plane, similar to Fig.11. Tracing the waveform shapes from the in-plane/upstream position to the downward/downstream direction, it is highly interesting to see how the advancing side BVI gradually vanishes and the retreating side BVI appears. The polar diagram inserted in the center of Fig. 13 using the BVI peak-to-peak values as a characteristic measure clearly illustrates the directivity of advancing and retreating side BVI. The retreating side BVI is expectedly of lower amplitude,because the retreating side blade tip

Mach-number is considerably smaller than on the advancing side. The maximum intensity of retreating side BVI is radiated at about 30 degree down from the rotor plane in downstream direction.

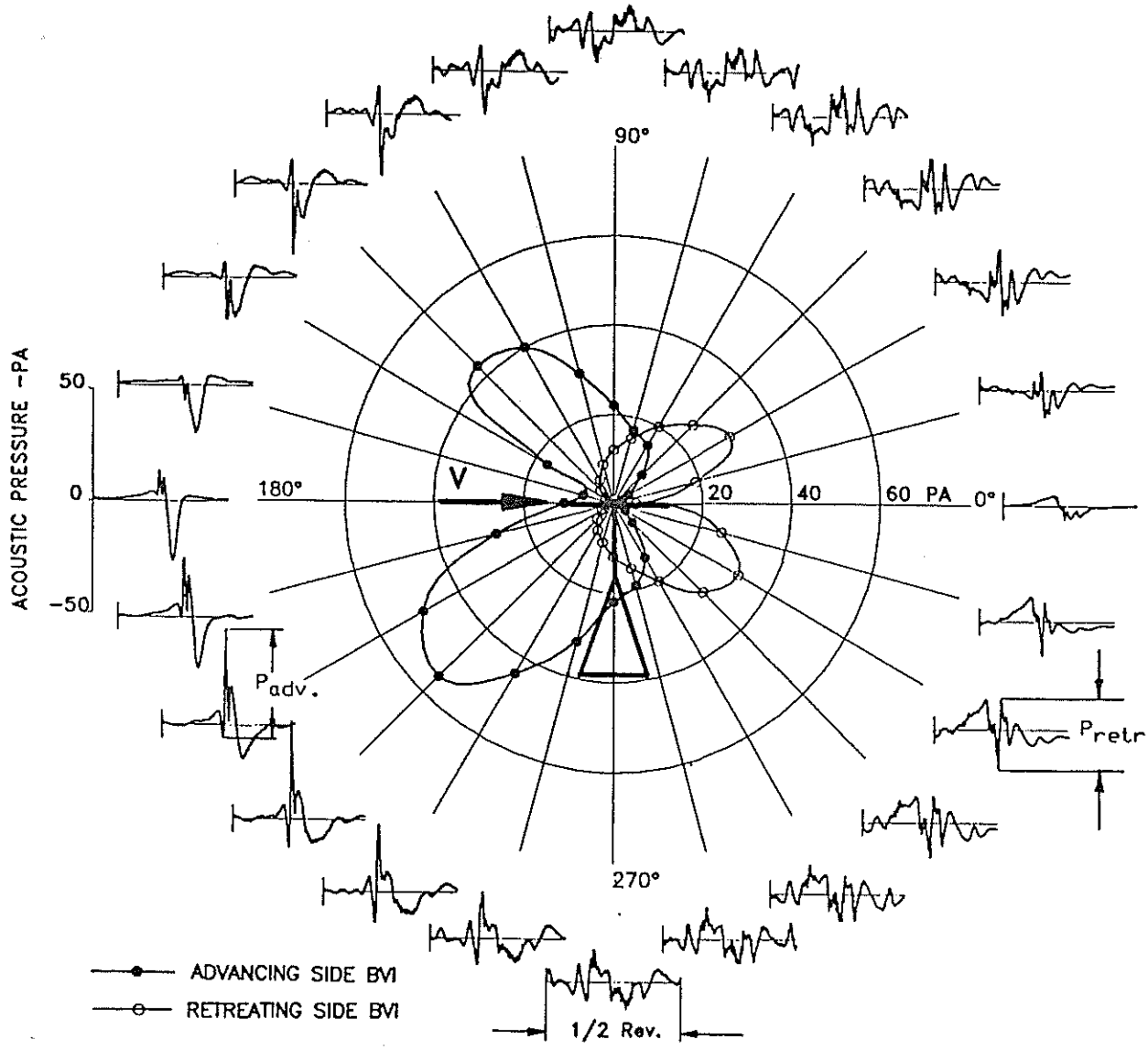

Fig.13: Predicted polar directivity characteristics vertical to the rotor plane at BVI condition showing advancing and retreating side BVI radiation lobes

It is interesting to note that both advancing and retreating side BVI are also radiated above the rotor disk, with radiation lobes that are symmetrical to the rotor plane in a first approximation. For both advancing and retreating side BVI a change in polarity of the BVI peak amplitudes takes place. This is in agreement with the experimental finding for a microphone location above the rotor plane, as was reported in Ref. 14.

The polar diagram of Fig.13 also shows that the intensity of advancing and retreating side BVI above the rotor plane is lower than below the rotor plane. This might be explained by a different superposition of the thickness and the loading term (phase differences).

The time history plots for locations vertical above and below the rotor plane in Fig.13 finally illustrate the appearance of alternating positive and negative pressure spikes also observed by other researchers(Ref.21).

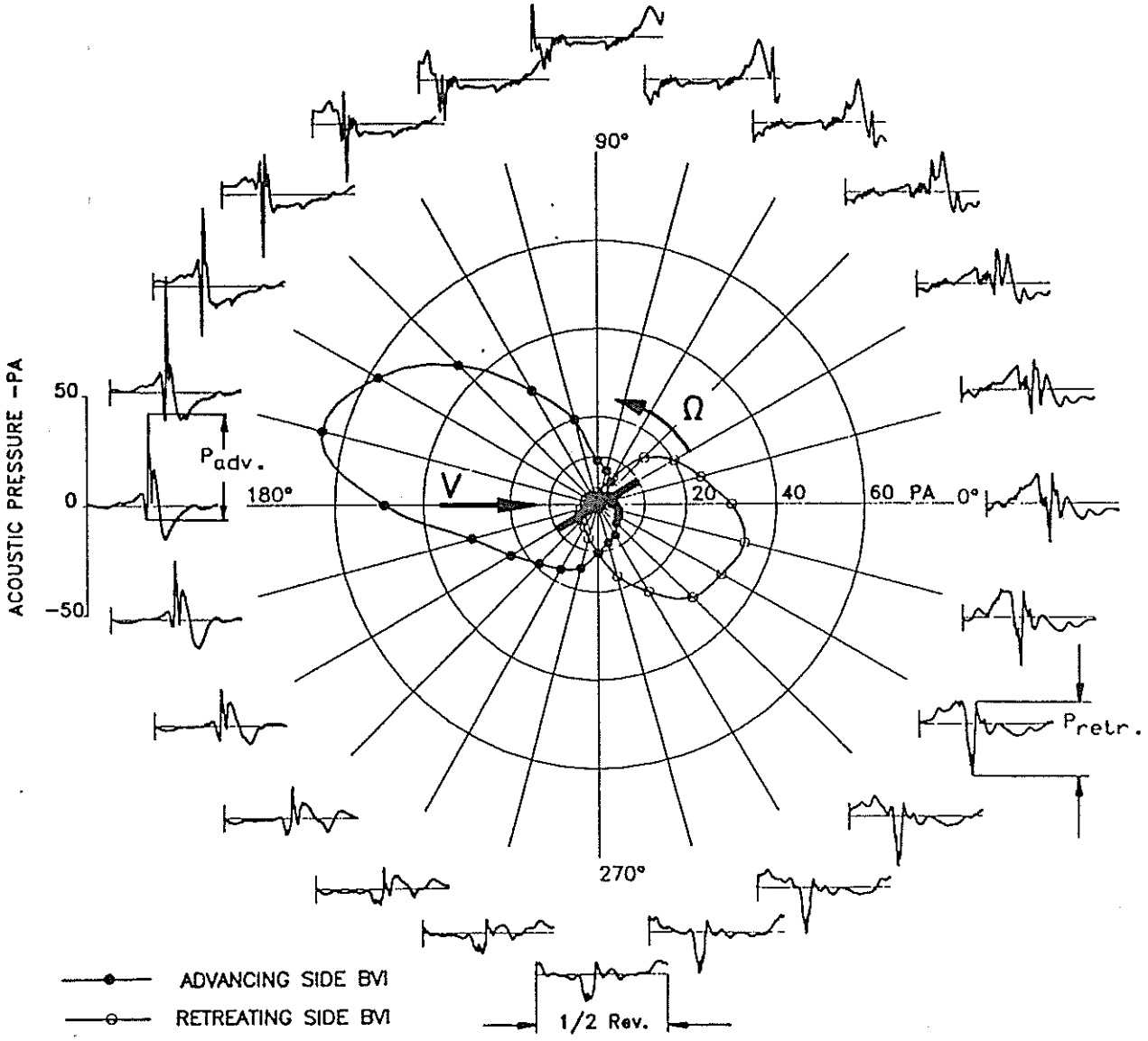

Fig.14: Predicted lateral directivity characteristics in the horizontal plane 30 degrees below the rotor plane at BVI condition

Fig.14 shows the lateral BVI directivity characteristics in a plane below the rotor disk for a full circle 30 degrees down from the rotor hub. Also in this plot the decreasing of advancing side BVI and the increasing of retreating side BVI in the downstream direction is visible. Again it is obvious that the amplitudes for retreating side BVI are less than for advancing side BVI. The most intense BVI radiation in this plane below the rotor disk is observed for an azimuth angle of about 165 degrees. This is in agreement with the experimental finding for this rotor (Ref.17).

7. Conclusions

A new attempt was made to use measured model rotor blade surface pressure data as source input for a prediction code including all of the three source terms of the "FWH"-equation. The measured blade pressure data were directly used as input for the loading term by means of a special interpolation scheme, and in a more indirect manner to calculate an approximated quadrupole term, which cannot be neglected at high tip Mach-numbers.

The prediction code was first applied to a well-documented hover condition. The predicted acoustic waveforms and spectra were shown to be in excellent agreement with the experimental findings up to tip Mach-numbers of about 0.92.

The prediction for two forward flight high-speed noise conditions and for one descending flight condition with strong BVI activity were compared with measured model rotor noise data. Good agreement in waveforms and directivity could be demonstrated.

Longitudinal and lateral directivity characteristics of high speed impulsive noise radiation were predicted and shown for the complete radiation angle ranges. The strong in-plane/upstream directivity could be illustrated. It was found that the predicted directivity at high tip Mach-numbers was slightly different from the experimental finding. To further improve the agreement of theory and experiment the quadrupole approximation has to be supplemented by exact near-field aerodynamic calculations and probably by the inclusion of dynamic effects of the rotor blades.

The complete lateral and longitudinal directivity characteristics of BVI impulsive noise were calculated. In addition to the advancing side BVI in the upstream radiation field, the development of retreating side BVI in the downstream/down radiation field was clearly demonstrated. For both advancing and retreating side BVI the change of polarity of the BVI peak amplitudes in the radiation field above the rotor plane was illustrated.

8. References

1. Ffowcs Williams, J.E. and Hawkings, D.L., Sound Generated by Turbulence and Surfaces in Arbitrary Motion, Philos. Trans. R.Roc London, Ser.A, Vol. 264, pp. 321-342, May 1969.

2. Farassat, F., Theory of Noise Generation from Moving Bodies with an Application to Helicopter Rotors, NASA TR R-451, Dec. 1975.

3. Boxwell, D.A., Yu, Y.H., and Schmitz, F.H., Hovering Impulsive Noise: Some Measured and Calculated Results, NASA CP-2052, 1978, and Vertica, Vol. 3, No. 1, 1979.

4. Farassat, F., Nystrom, P.A., and Morris, C.E.K., Jr., A Comparison of Linear Acoustic Theory with Experimental Noise Data for a Small Scale Hovering Rotor, AIAA Paper 79-0608, Seattle, Wash., 1979.

5. Brentner, K.S., A Prediction of Helicopter Rotor Discrete Frequency Noise for Three Scale Models Using a New Acoustics Program, AIAA 25th Aerospace Science Meeting, Reno, Nevada, 1987.

6. Yu, Y.H., Caradonna, F.X., and Schmitz, F.H., The Influence of the Transonic Flow Field on High-speed Helicopter Impulsive Noise, 4th European Rotorcraft and Powered Lift Aircraft Forum, Paper No 58, Italy, 1978.

7. Schmitz, F.H. and Yu, Y.H., Transonic Rotor Noise - Theoretical and Experimental Comparisons", Vertica, Vol. 5, pp. 55-74, 1981.

8. Prieur, J., Calculation of Transonic Rotor Noise Using a Frequency Domain Formulation, 43th AHS-Forum Poceedings. pp. 469-479, St. Louis, Missouri, 1987.

9. Caradonna, F.X., The Transonic Flow on a Helicopter Rotor, Ph. D. Dissertation, Stanford Univ., Calif., 1978.

10. Chattot, J.J., Calculation of Three-dimensional Unsteady Transonic Flows Past Helicopter Blades, NASA Techn. Paper No 1721, AVRADCOM Techn. Report 80-A-2, 1980

11. Nakamura, Y., Prediction of Blade-vortex Interaction Noise from Measured Blade Pressure, 7th European Rotorcraft and Powered Lift Aircraft Forum, Paper 32, Garmisch-Partenkirchen, Federal Republic of Germany, 1981.

12. Ziegenbein, P.R. and Oh, B.K., Blade- vortex Interaction Noise Predictions Using Measured Blade Surface Pressures, AHS Specialists' Meeting on Aerodynamic and Aeroacoustics, Arlington, Texas, Febr. 1987.

13. Joshi, M.C., Lin, S.R., and Boxwell, D.A., Prediction of Blade Vortex Interaction Noise, 43th AHS-Forum Proceedings, pp. 453-460. St. Louis, Missouri, 1987.

14. Schultz, K.J., Splettstoesser, W.R., Prediction of Helicopter Rotor Impulsive Noise Using Measured Blade Pressures, 43th AHS-Forum Proceedings, pp. 405-420, St. Louis, Missouri, 1987.

15. Schmitz, F.H., Yu, Y.H., Theoretical Modelling of High Speed Helicopter Impulsive Noise, J. Amer. Helicopter Soc., 1979.

16. Farassat, F. and Brentner, K.S., The Uses and Abuses of the Acoustic Analogy in Helicopter Rotor Noise Prediction, Paper presented at the AHS National Specialists' Meeting on Aerodynamics and Aeroacoustics, Arlington, Texas, Febr. 1987.

17. Splettstoesser, W.R., Schultz, K.-J., Boxwell, D.A., and Schmitz, F.H., Helicopter Model Rotor-blade Vortex Interaction Impulsive Noise: Scalability and Parametric Variations, 10th European Rotorcraft Forum, Paper No 18, The Hague, The Netherlands, Aug. 1984.

18. Splettstoesser, W.R., Schultz, K.-J., Schmitz F.H., and Boxwell, D.A., Model Rotor High Speed Impulsive Noise - Parametric Variations and Full-scale Comparisons, 39th Annual National Forum of the American Helicopter Society, Paper No 53, St. Louis, Mo., May 1983.

19. Boxwell, D.A., Schmitz, F.H., Splettstoesser, W.R., and Schultz, K.-J., Model Helicopter Rotor High Speed Impulsive Noise - Measured Acoustics and Blade Pressures, NASA Technical Memorandum 85850 and USAAVRADCOM Technical Report-83-A-14, Sept. 1983.

20. Boxwell, D.A., Schmitz, F.H., Splettstoesser, W.R., and Schultz, K.-J., Lewy, S., Caplot, M., A Comparison of the Acoustic and Aerodynamic Measurements of a Model Rotor Testes in Two Anechoic Wind Tunnels, 12th European Rotorcraft Forum, Paper No 38, Garmisch-Partenkirchen, Sept. 1986.

21. Hubbard, J.E. and Leighton, J.E., A Comparison of Model Helicopter Rotor Primary and Secondary Blade/Vortex Interaction Blade Slap, AIAA 8th Aeroacoustics Conference, Paper No AIAA-83-0723, 1983.